Carbon-based composite electrodes C – TiC/TiB_2. Part 1. Synthesis and oxidizability of composites

E. S. Gorlanov*, *Deputy Director, Scientific Center for Problems of Processing of Mineral and Technogenic Resources*[1], *e-mail: Gorlanov_ES@pers.spmi.ru*
V. M. Sizyakov, *Professor, Scientific Director, Scientific Center for Problems of Processing of Mineral and Technogenic Resources*[1], *e-mail: Sizyakov_VM@pers.spmi.ru*
F. Yu. Sharikov, *Chief Researcher, Scientific Center for Problems of Processing of Mineral and Technogenic Resources*[1], *e-mail: Sharikov_FYu@pers.spmi.ru*
K. D. Shaikina, *Master's Student, Scientific Center for Problems of Processing of Mineral and Technogenic Resources*[1], *e-mail: shaikinaksenia@yandex.ru*
O. A. Mozulev, *Master's Student, Scientific Center for Problems of Processing of Mineral and Technogenic Resources*[1], *e-mail: Mozulev_OA@pers.spmi.ru*

[1] *Empress Catherine II Saint Petersburg Mining University, Saint Petersburg, Russia.*

The main results of a lab-scale technological development of a composite material "Carbon – Titanium Carbide/Titanium Diboride" (C – TiC/TiB_2) carbothermal synthesis are presented in the work. Initial components – petroleum coke of various fractional compositions, titanium and boron compounds together with the binder – were mixed and calcinated at 1050 °C in air under the layer of preliminarily calcinated coke. Composite material C – TiC/TiB_2 synthesized this way demonstrated a rather high resistivity to oxidation in air. In our mind the result was reached due to the formation of a Ti – C – B – O bonding medium on the surface and between the grains of a carbon material. It was found that resistivity to oxidation and degradation under various temperatures can be controlled with glass boron oxide fine condition, its distribution over the surface and with the rate of its evaporation from the electrode surface. An overall mechanism of the composite electrode oxidation process was proposed and the corresponding kinetic parameters of weight loss rate as a function of temperature were found. The proposed technological procedure of composite electrodes formation may be applied for a wide range of C – MeC/MeB_2 based materials, including electrodes for arc steel-smelting and ore-thermal furnaces, magnesium and aluminium cells.

Key words: composite material, C – TiC/TiB_2 composition, oxidation rate, activation energy.
DOI: 10.17580/nfm.2024.02.03

Introduction

Carbon materials are widely applied in various metallurgical processes and technological units, where they should work in highly aggressive media for a long time and retain their functional characteristics. It is obvious that the corresponding initial carbon materials [1–3], their fractions [4, 5], bonding materials and modifying agents should meet very strict characteristics in composition [6–8], emissions of gaseous and solid components [9–11].

Graphitized and coal electrodes of ore-thermal furnaces [12, 13], as well as magnesium cell anodes [14, 15] – are subject both to thermal shock and high-temperature oxidation. These electrodes are often protected via impregnation with coal peck [16–18] and special solutions [19–21] or melts [22] that retard oxidation. Ceramic coatings made of aluminum [23–25], titanium [26–28], silicon [29–31], chromium [32, 33] oxides or carbides are also used. These technological operations do improve the electrodes resistivity to oxidation and degradation, but the effect is mainly noticeable at the beginning of an electrode working cycle. The reason is that the electrode surface and volume close to surface are only protected this way, and anyway the near-surface layer is being oxidized with gaseous oxidation products formation, it finally loses its mechanical integrity that results in an electrode degradation and material sloughing. Ceramic coatings seem to be more reliable, but they are being flaked off in the result of numerous consecutive processes of thermal expansion and shrinkage. Similar problems are vital for carbon cathode blocks of aluminium electrolyzers that are subject to destruction with sodium ions and abrasive solid particles that are present in circulating melts [34–36].

Aim of the work is developing a basic scientific and technological approach to synthesis and production of a composite electrode material with improved operating characteristics in course of a standard calcination procedure of carbon materials that is performed at 1000–1100 °C under the coke layer or in an inert atmosphere.

Thermodynamic argumentation

To synthesize a perfect composite material resistant at a high temperature in aggressive atmosphere for a long time — one needs not only to perform an appropriate

*Correspondence author.

mechanical mixing of initial carbon material with dopants or their precursors, but also to provide their location and necessary chemical interactions in intercrystalline space of a final electrode [37]. Transition metal oxides may be used as dopant precursors with their further transformation to highly resistant metal-carbon compounds at an elevated temperature. In case of applying TiO_2 as a precursor the estimation is as follows. According to thermodynamic data their synthesis, e.g., titanium carbide TiC or titanitum diboride TiB_2, is possible only at temperature 2000 °C and higher, and not at 1000–1100 °C as we need:

	ΔG^0_{3100}, kJ/mol	ΔG^0_{1300}, kJ/mol	
$TiO_{2(s)} + 2C_{(s)} = TiC_{(s)} + 2CO_{(g)}$	–241.0	118.12	(1)
$TiO_{2(s)} + B_2O_{3(g)} + 5C_{(s)} \rightarrow TiB_{2(s)} + 5CO_{(g)}$	–624.0	+41.21	(2)

In case that we are limited with the 1000–1100 °C interval — standard for carbon material thermal treatment – the solution may be in applying dispersed metal Ti as a precursor to synthesize TiC and TiB_2 in course of the following exothermal reactions with the negative ΔG^0 values [38]:

$$Ti + C = TiC \qquad \Delta G^0_{1300} = -168.64 \text{ kJ/mol} \quad (3)$$

$$Ti + B_2O_3 + 3C \rightarrow TiB_2 + 3CO \qquad G^0_{1300} = -41.13 \text{ kJ/mol} \quad (4)$$

We suppose that reactions (3)–(4) may be run completely at a prolonged calcination of a composite material at 1000–1100 °C and final reaction products (TiC, TiB_2) located at the surface and in the intercrystalline space of a final electrode will make it highly resistant in an aggressive medium.

Experimental section

Preparing a composite electrode sample

A standard procedure was applied for mixing the initial components, the green electrode formation and its further calcination. Petroleum coke with particles <2 mm and coal pitch (13–15 wt.%) were mixed in a mixer at an elevated temperature (135 ± 5 °C) for 15–20 min. A mixture of Ti, TiO_2 and B_2O_3 was then added in a quantity up to 45%wt. to the mixture of petroleum coke and pitch. All reagents were of chemically pure grade.

The green electrode samples were formed in a heated matrix (~120 °C) in the form of cylinders D = 30 mm and H = 30–50 mm with applying static pressure ~15.0 MPa. After that they were calcinated for 3 h in a muffle furnace at temperature 1050 ± 10 °C in air under the layer of a calcinated petroleum coke to prevent oxidation. Simulation of carbon materials calcination procedure in an industrial furnace with the possibility of a partial oxidation of the protective compounds being synthesized was done this way.

Oxidation study of the composite electrode samples and data presentation

A comparative testing of various electrodes in oxidative atmosphere was done. Graphite electrodes and those made of petroleum coke and protected with TiC/TiB_2 compounds were studied. Some of graphite electrodes were additionally impregnated with a mixture of phosphoric and boron acids under vacuum to make them more stable and compare with composite electrodes. Effective density and open porosity of all electrodes to be tested were within 1.56–1.61 g/cm^3 and 19–25%, respectively. Relative stability testing of various electrodes was done in static air atmosphere in a muffle furnace (LOIP, Russia) under isothermal conditions at 520, 710, 820, 920 and 1050 °C **(Fig. 1)**. Heating rate 5 °C/min from ambient temperature to a testing temperature was applied. Total duration of an electrode test at each temperature was from 20 to 30 h as a consequence of 5 h intervals (heating to a selected T_{iso} — 5 h under isothermal conditions – cooling to ambient T — weight loss and geometrical dimensions measuring).

Analytical balance and digital slide gauge were used. Specific weight loss at a single time interval and for the whole consequence was done according to the following formula:

$$\frac{\Delta m}{S} = \sum_{i=0}^{n} \frac{m_n - m_{n-1}}{S_n}, \text{ mg/cm}^2 \quad (5)$$

where m_n and m_{n-1} – sample weight before and after the test; n – number of a single test interval; S_n – geometrical surface value before a single test interval (5 h), cm^2.

Specific oxidation rate ΔV as a function of time interval $\Delta\tau$ is as follows:

$$\Delta V = \frac{\Delta m}{S_n \cdot \Delta\tau}, \text{ mg/cm}^2 \cdot \text{h} \quad (6)$$

The experimental results were presented in a graphic form for further analysis and discussing the possible overall mechanism of the composite electrodes oxidation depending on their prehistory. The data were fitted as functions $\Delta m/S = f(\tau)$ or $\Delta m/S \cdot \tau = f(\tau)$ with a regression coefficient $R^2 \geq 0.95$. In most cases the condition was fulfilled. It may be

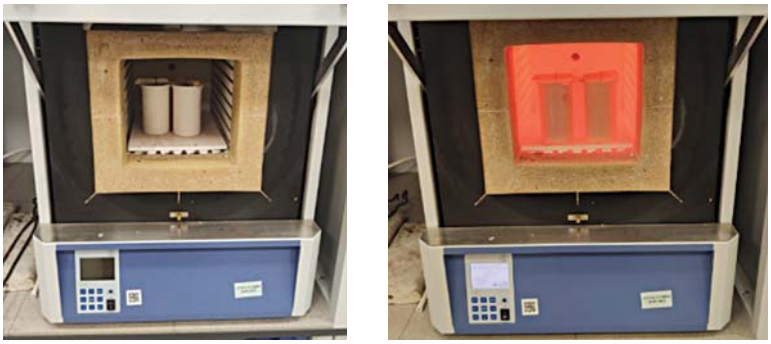

Fig. 1. LOIP muffle furnace with the loaded samples (in ceramic crucibles) in course of the oxidative test

considered as a fact that the electrode oxidation process is controlled with the sample surface value and a mixed mode of oxidation reaction rate together with the outer diffusion process rate of oxidation products:

$$(\Delta m/S)^n = K_n\tau \text{ , mg/cm}^2 \quad (7)$$

where K_n is the rate constant of oxidation reaction; n — exponent; τ — oxidation time.

There may be two utmost variants of running the oxidation process in accordance with the equation (8). At $n < 1$ and at n approaching to 1.0 oxidation rate is mainly defined with interaction of oxygen with the material. We suppose that at $1 < n \leq 2$ the limiting stage of overall electrode oxidation process rate is changing from mainly kinetic one ($n \geq 1$) to mainly diffusional one ($n \leq 2$) (oxygen diffusion to the reaction surface through the gaseous oxidation products).

The regression equations used for the data kinetic analysis are as follows:

$$\Delta m/S = K_T \cdot \tau^a \qquad n = 1/a \quad (8)$$

$$\Delta m/S \cdot \tau = K_V \cdot \tau^{-m} \qquad n = 1/1 - m \quad (9)$$

where K_T and K_V – rate constants of the oxidation reaction that have dimensions depending on the values of a and m parameters, respectively. Temperature dependency of the rate constants at a given oxygen partial value is expressed via the well-known Arrhenius equation:

$$K_{T,\,V} = K_0 \cdot exp\left(\frac{E_a}{RT}\right) \quad (10)$$

where E_a – effective activation energy of oxidation reaction, J/mol; R – universal gas constant, J/(mol · K); T – temperature, K; K_0 – pre-exponential factor, it does not depend upon temperature.

Linearization of the functions $\Delta m/S = f(\tau,\ T)$ and $K_{T,\,V} = f(\tau)$ was performed in a usual way via transforming equations (8)–(10) to a logarithmic form. Rate constants were presented in mg/cm^2 · h.

Electrode samples instrumental analysis

The carbon composite samples were analyzed after each heating procedure (synthesis at 1050 °C, oxidation testing) with applying XRD technique (XRD-7000 by Shimadzu, Japan) and/or SEM with EDX local analysis (Vega 3 LMH by TESCAN, Czech Republic).

Results and discussion

Synthesis of composite electrodes

XRD analysis data of the composite C – TiC/TiB_2 synthesized at 1050 °C are presented in **Fig. 2.** Initial charge had the composition {76C + 8TiO_2 + 16(Ti + B_2O_3)}[1]. The main phase is predictably identified as carbon, and other phases with lower intensity are presented with Ti and B compounds — titanium borides and carbides, such as TiB_2, TiB, TiC_x — that were generated in accordance with reactions (1) – (4).

Oxygen-containing compounds — titanium borate $TiBO_3$, oxides of titanium (TiO_2) and boron (B_2O_3) — are supposed to be the products of titanium borides partial oxidation in course of the synthesis procedure. One might expect the presence of boron oxide in composites **(Fig. 3)**, its absence in some materials may be explained with its evaporation and/or consumption due to (3) and (4) reactions in course of synthesis **Fig. 2.**

The synthesis result is supposed to be mainly dependent upon Ti/B_2O_3 fraction in the initial charge. If we increase B_2O_3 content — it appears in the final composite in a noticeable amount **(**see **Fig. 4).**

The presence of boron oxide at the composite surface was directly confirmed with SEM-EDX analysis **(**see **Fig. 5)**. B_2O_3 forms a continuous layer of micro-bubbles located at the surface. That may be the result of its partial evaporation at the synthesis temperature (1050 °C) together with other volatile products generation according to (1) – (4) reactions.

The presence of boron oxide at the composite surface might indicate that one could provide optimal conditions for generating the essential oxidation-resistant phases TiB_2, Ti_2B_5, TiB, TiC_xO_{1-x}, $TiBO_3$ **(**see **Fig. 6)** via changing the Ti/B_2O_3 fraction in an initial charge.

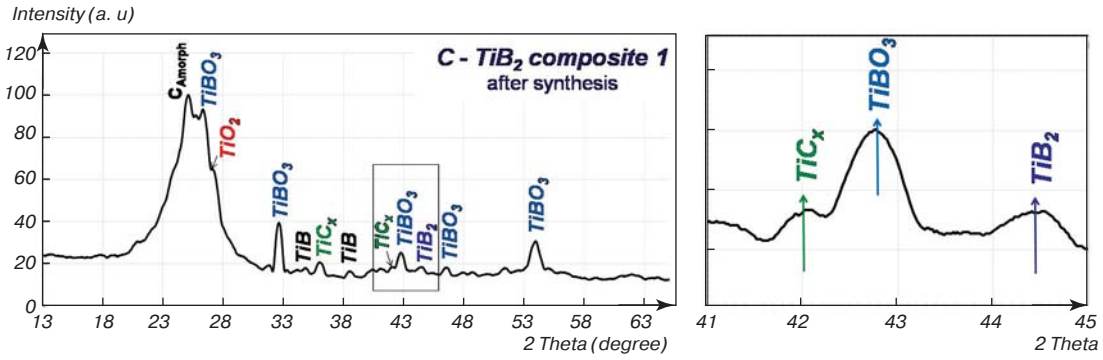

Fig. 2. XRD analysis results of {76C + 8TiO_2 + (16Ti+B_2O_3)$^{№1}$} composite after synthesis

[1] Initial charge composition prepared for composites synthesis is given in wt.%.

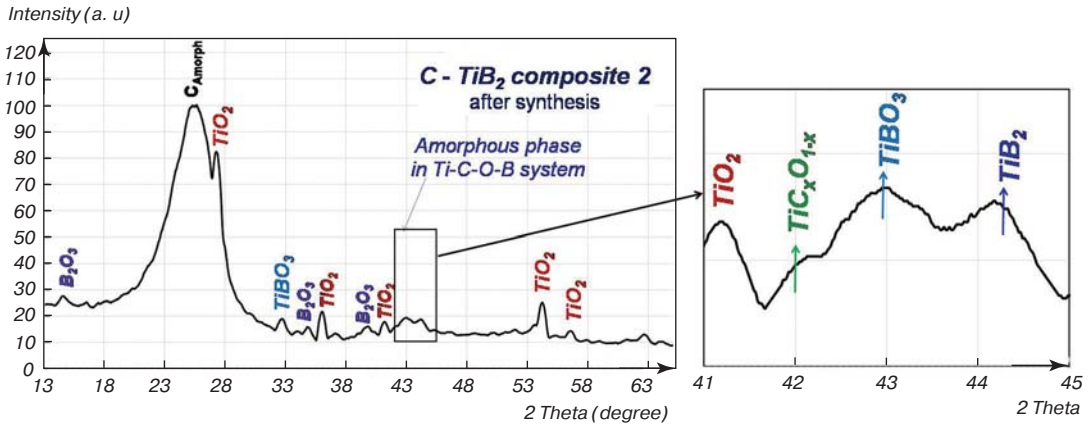

Fig. 3. XRD analysis results of {80C + 20(Ti + B_2O_3)$^{№2}$} composite after synthesis

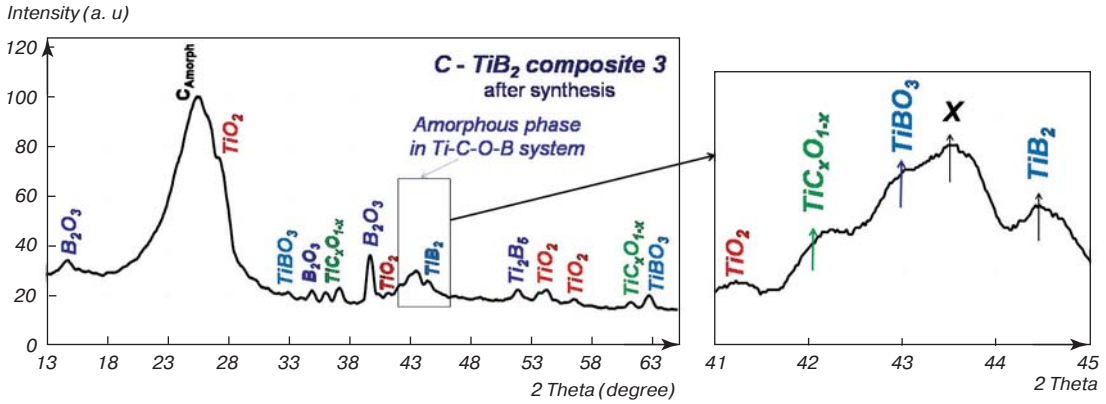

Fig. 4. XRD analysis results of {70C + 30(Ti + B_2O_3)$^{№3}$} composite after synthesis

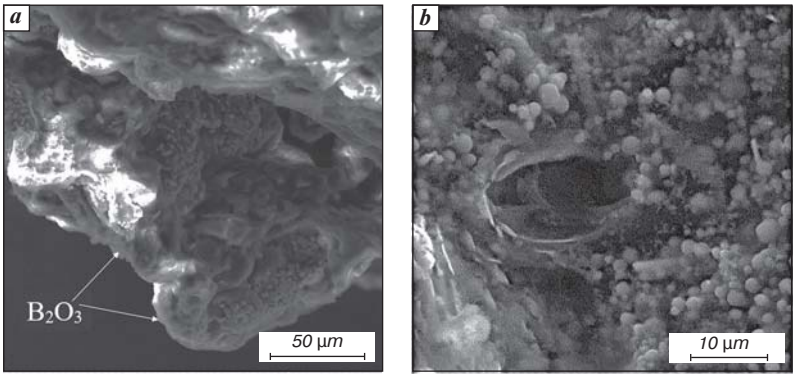

Fig. 5. SEM analysis results of {70C + 30(Ti + B_2O_3)$^{№3}$} composite after synthesis: *a* – boron oxide layer at the surface, *b* – boron oxide bubbles (a greater magnification)

One should emphasize an amorphous phase with a wide XRD peaks profile within the range 41–45° (2θ). This range is additionally selected and enlarged with the corresponding rectangles in **Figs. 2–6**. At scaling this range one could suppose the presence of phases TiC_xO_{1-x}, TiC and TiC_x (42.0–42.3°), $TiBO_3$ (42.9°), TiB2 (44.5°). The presence of a phase (or a number of phases) containing Ti, C, B and O was shown with applying SEM-EDX analysis in the volume of electrode samples **(Fig. 7, Table 1)**.

We suppose that these are the complex phases or their non-stoichiometric Ti – C – B – O derivatives. Their possible formation may be presented with the following reactions (11–12):

$$TiB_2 + TiO_2 \rightarrow TiB_2 \times TiO_2 \rightarrow Ti_xB_yO_z \quad (11)$$

$$TiB_2 + TiC_xO_{1-x} = \\ = TiB_2 \times TiO_2 \times TiC \rightarrow Ti_xB_yC_zO_k \quad (12)$$

These not properly crystallized complex phases of Ti – C – B – O composition found at the surface and between crystallites may be considered as a source of improving the electrodes resistance in an aggressive oxidizing medium.

Relative oxidation rate of composite electrode samples

A comparative test of various electrodes behavior under oxidation was performed in order to better estimate the possible advantages of composite electrodes. Composite electrodes were compared with the traditional graphite electrodes and also with those impregnated with an aqueous mixture of phosphoric and boric acids **(Fig. 8)**.

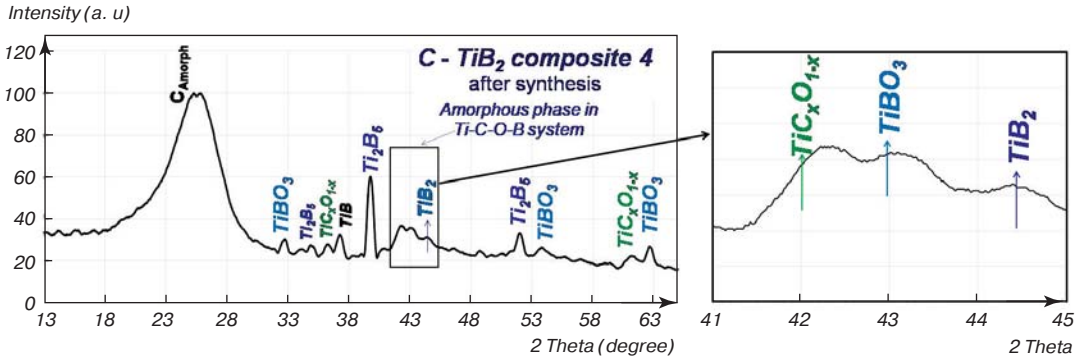

Fig. 6. XRD analysis results of {60C + 40(Ti + B2O3)$^{№4}$} composite after synthesis

The least resistance to oxidation under the test conditions (710 °C, static air) was predictably demonstrated by an ordinary graphite electrode. Impregnation of graphite electrode does noticeably reduce its oxidation rate compared to a non-impregnated one – but only for the initial period around 10–15 h. After this time the oxidation rate of an impregnated electrode becomes similar to that for a non-impregnated one **(Fig. 8)**. Oxidation dynamics of both kinds of graphite electrodes is described with exponential regression equations with a high correlation coefficient $R^2 = 0.96–0.99$. It may be concluded that the oxidation reaction rate in a stationary mode for the tested materials is controlled with a direct interaction of oxygen with carbon.

The fundamental difference the dynamics of mass loss of C – TiC/TiB_2 electrodes is the decrease in the oxidation rate during testing, which is described by power equations (8) of the regression curve **(Fig. 8)**. The exponent value $n = 1/a$ is within the 1.2–1.4 interval that may indicate of a mixed mode of the oxidation rate control including both chemical kinetics and diffusion. Competition of chemical and diffusional processes in the overall oxidation process may be explained with the presence of individual phases TiB_2, TiB, TiC_x, $TiBO_3$ and probably complicated amorphous phases of Ti – C – B – O composition **(**see **Fig. 9).**

We suppose that TiC_x, TiB, and TiB_2 phases generated inside and at the surface of the synthesized composite electrode sample are transformed to titanium oxides TiO and TiO_2 together with the glass B_2O_3 phase formation in course of the 30 hour oxidation test **(Fig. 9)** according to the following equations:

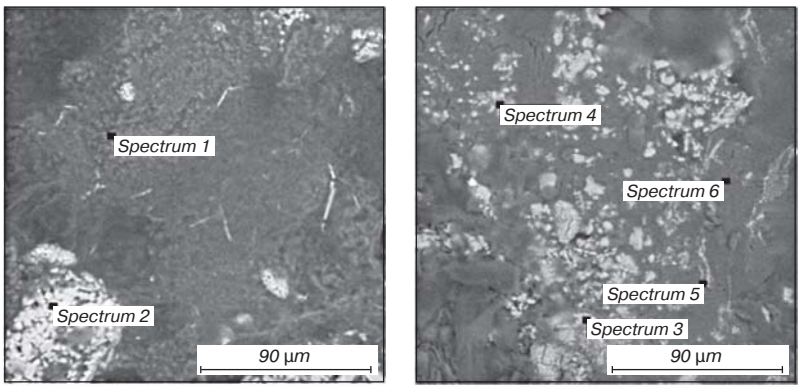

Fig. 7. SEM-EDX local spectral analysis data of {70C + 30(Ti + B_2O_3)} composite after synthesis (areas within the volume of an electrode sample)

Table 1

EDX elemental analysis results of {70C+30(Ti+B_2O_3)$^{№3}$} compos

No. of a point at the image	Elemental composition, atomic %				Possible phase
	Ti	C	B	O	
1	0.10	53.38	44.13	2.39	Ti – C – B – O
2	35.60	8.95	20.82	34.63	
3	9.58	11.67	6.21	72.54	
4	9.75	32.62	7.14	50.49	
5	11.13	26.38	5.22	57.27	
6	11.66	–	–	88.34	TiO_2

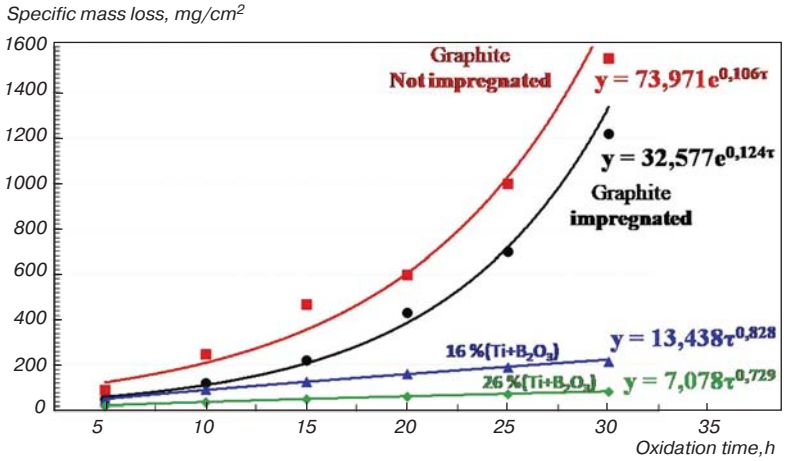

Fig. 8. Oxidation kinetics of a traditional graphite electrode, a graphite impregnated electrode and composite electrodes of two kinds — {84C + 16(Ti + B_2O_3)} and {74C + 26(Ti + B_2O_3)} — at 710 °C in static air atmosphere

	ΔG^0_{1300}, kJ/mol	
$TiB_2 + 5/2O_2 \rightarrow TiO_2 + B_2O_{3(l)}$	−1345.83	(13)
$TiB_2 + 2O_2 \rightarrow TiO + B_2O_{3(l)}$	−1056.57	(14)
$TiB_2 + 9/2O_2 = TiBO_3 + 1/2B_2O_3$	−561.51	(15)
$TiB_2 + 9/4CO_2 = TiBO_3 + 1/2B_2O_3 + 9/4C$	−315.05	(16)
$TiB_2 + 9/2CO = TiBO_3 + 1/2B_2O_3 + 9/2C$	−187.50	(17)

Oxidation and transformation of $TiBO_3$ phase in the synthesized composite may be presented with the following equations:

	ΔG^0_{1300}, kJ/mol	
$TiBO_3 + 1/2CO = TiO_2 + 1/2B_2O_3 + 1/2C$	−211.18	(18)
$TiBO_3 + 1/4O_2 = TiO_2 + 1/2B_2O_3$	−139.53	(19)
$TiBO_3 + 1/4CO_2 = TiO_2 + 1/2B_2O_3 + 1/4C$	−40.51	(20)

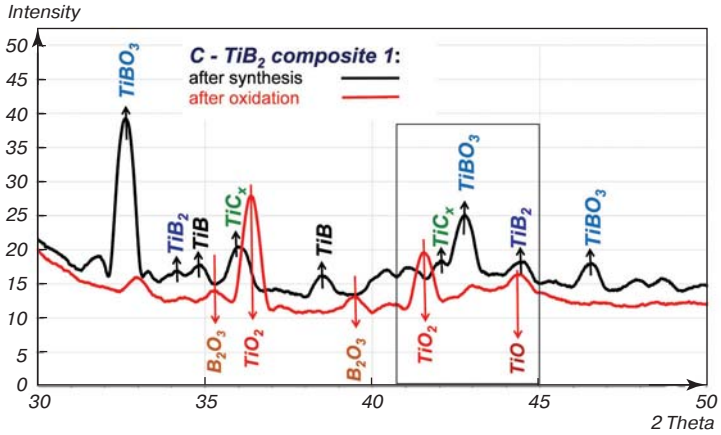

Fig. 9. XRD analysis results of $\{76C + 8TiO_2 + 16(Ti + B_2O_3)^{№1}\}$ composite after synthesis and consequent oxidation for 30 h at 710 °C in static air atmosphere

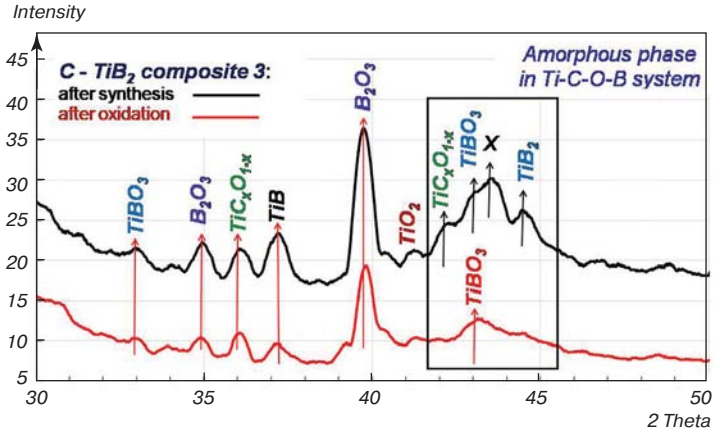

Fig. 10. XRD analysis results of $\{70C + 30(Ti + B_2O_3)^{№3}\}$ composite after synthesis and consequent oxidation for 30 h at 710 °C in static air atmosphere

A continuous layer of B_2O_3 is formed at the composite surface after synthesis in case of a relatively high content of boron oxide in the initial charge. This layer is remained at the sample surface in cause of the oxidation test, at least for the first 30 hours **(Fig. 10)**.

Some individual phases, such as TiB, $TiBO_3$, are partially remained as the protective ones, and they may also serve as a source of glass B_2O_3 phase generation. Amorphous phases of Ti – C – B – O composition is partly remained, but it is mainly transformed to the titanium borate phase $TiBO_3$ **(Fig. 10)**.

These results make it possible to formulate the main reason of a relatively high oxidative resistance of composite electrodes at elevated temperatures in air — a dense mixture of various phases of Ti – C – B – O composition between the carbon grains (see **Figs. 9, 10**) is working as an active protective component. It makes the composite electrode rather more resistant to oxidation and degradation compared to an ordinary graphite electrode.

The mechanism of composite electrodes oxidation

The experimental results of testing various composite electrode samples in static air atmosphere at different temperatures and initial concentrations of Ti and boron oxide are given in **Fig. 11.** Data of oxidation experiments were treated with applying the function of specific weight loss $\Delta m/S = f(\tau)$. In experiments run at 710 °C the n values in the approximation function are diminished from 1.37 to 0.99 at decreasing the $(Ti + B_2O_3)$ fraction from 26 to 13%, respectively. It may indicate of a change in the character of oxidation from a mixed mode (both diffusion and kinetics) to a linear one **(Fig. 11, *a*)**.

The same dependency is observed at 820 °C, but the kinetic mode of oxidation is observed for the composite with 16 wt.% of $(Ti + B_2O_3)$ fraction in initial charge **(Fig. 11, *b*)**. If we pass to the oxidation experiments at 920 °C — the composite sample weight loss becomes linear in spite of increasing the $(Ti + B_2O_3)$ fraction in initial charge to 30–45 wt.% **(Fig. 11, *c*, Table 2)**. At this temperature the composite sample oxidation process is supposed to be run in a kinetic mode.

The oxidation rate of composite electrode samples (ΔV, mg/cm^2 · h) is decreasing at increasing the weight fraction of $(Ti + B_2O_3)$ in initial charge from 13 to 45 wt.% in the studied range of oxidation temperatures (710–920 °C). The corresponding data related to oxidation study at 710 °C are presented in **Fig. 12**.

Oxidation rate decreasing with time that was indicated for all the electrode samples may be explained that the oxidation process is monitored not only with the resistance of C – Ti – B – O amorphous phases generated in cause of composite synthesis, but also with oxygen diffusion through the constantly increasing layer of glassy B_2O_3 at

the composite surface together with titanium oxides layer generation.

Preliminary conclusions on the oxidation mechanism of C – TiC/TiB_2 composites are confirmed with the experimental data on temperature dependency of specific weight loss in oxidation runs within temperature range 520–1050 °C **(Fig. 13)**.

Oxidation rate constant for composite electrode sample is increasing from ~2.70 (520 °C) to ~21.65 (1050 °C) with increasing temperature of isothermal runs (see **Fig. 13**). Oxidation rate of {74C + 26(Ti + + B_2O_3)} composite samples is increasing with temperature in the following way (see **Fig. 14**).

Oxidation rate of composite samples seems to retain a decreasing tendency in time up to almost 1000 °C. Exponential equations may be used for approximating these experimental data. Liquid boron oxide is supposed to form a continuous layer under these conditions (see **Fig. 15**), it is wetting the composite material framework — both C – B and C – Ti – B – O structures of a polycrystalline electrode sample.

Hence it may be concluded that up to 1000 °C the liquid B_2O_3 layer is working as a barrier for oxygen diffusion. Oxidation weight loss in this mode is monitored with a mixed mode of oxygen diffusion through this layer and oxygen interaction with the electrode material.

At temperatures higher that 1000 °C (e.g., at 1050 °C in our runs) oxidation rate decreasing is substituted with the opposite tendency of its progressive increasing due to the active B_2O_3 evaporation at a high temperature. Time point 10 h is the turning point under these conditions. Oxidation rate at 1050 °C is described with a polynomial equation **(Fig. 14)**. It means that the whole oxidation process is monitored only with the reaction of carbon with oxygen under these conditions.

An additional confirmation of changing the overall oxidation mechanism with temperature increasing is diminishing the exponent value "*n*" from 1.50 to 1.09. It may also indicate of changing the oxidation monitoring mode from a mixed one (both reaction kinetics and diffusion) to an almost linear one (see **Fig. 13** and **Table 3**).

The found kinetic parameters of composite materials oxidation **(Table 3)** also make it possible to evaluate the process effective activation energy. Temperature dependency of oxidation rate constant for composite {74C + 26(Ti + B_2O_3)} and temperature interval 520–1050 °C is presented in **Fig. 16**.

Two distinctive temperature intervals with two various effective activation energy values are obviously observed. A noticeable change of effective activation energy value around temperature 820 °C is in a good agreement with specific weight loss experimental data and oxidation rate data for the studied composite electrode samples in temperature

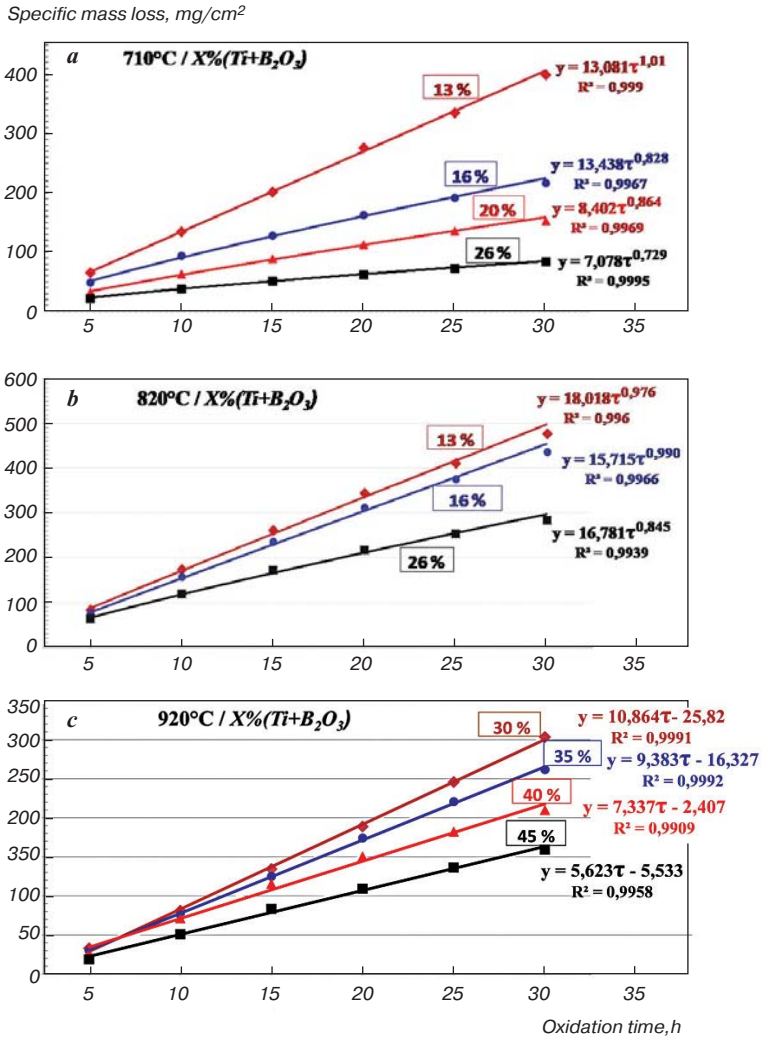

Fig. 11. Specific weight loss of composite electrode samples with various Σ(Ti + + B_2O_3) fractions at different temperatures in course of oxidation tests: *a* – at 710 °C – 13, 16, 20 and 26 wt.%; *b* – at 820 °C – 13, 16 and 26 wt.%, *c* – at 920 °C – 30, 35, 40 and 45 wt.%

Table 2

Kinetic parameters found for oxidation reactions of composite electrode samples after treatment of the experimental data presented in Fig. 11

Oxid. temp., °C	Σ(Ti + B_2O_3), wt.%	K_T	*a*	R^2	*n* = 1/*a*	Lim stage
710	13	13.081	1.01	0.999	0.99	*K*
	16	13.438	0.828	0.997	1.21	*D-K*
	20	8.402	0.864	0.997	1.16	*D-K*
	26	7.078	0.729	0.999	1.37	*D-K*
820	13	18.018	0,976	0.996	1.02	*K*
	16	15.715	0.990	0.997	1.01	*K*
	26	16.781	0.845	0.994	1.18	*D-K*
920	30	10.864	–	0.999	–	*K*
	35	9.383	–	0.999	–	*K*
	40	7.337	–	0.991	–	*K*
	45	5.623	–	0.996	–	*K*

Note: *K* – kinetic mode of oxidation reaction; *D-K* – mixed diffusional-kinetic mode of oxidation

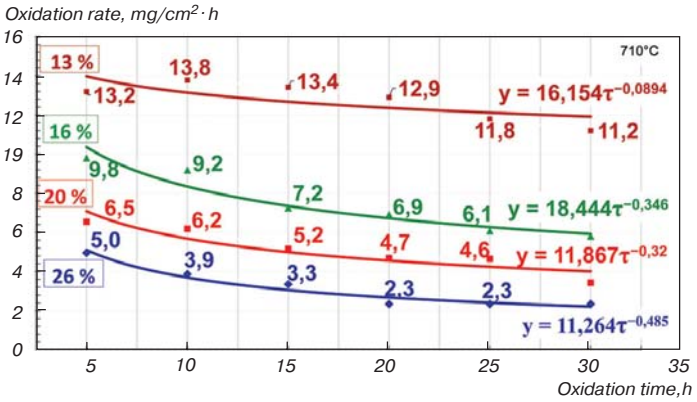

Fig. 12. Oxidation rate of composite electrode samples with the initial charge composition from {87C + 13(Ti + B_2O_3)} to {74C + 26(Ti + B_2O_3)} under isothermal conditions at 710 °C in static air

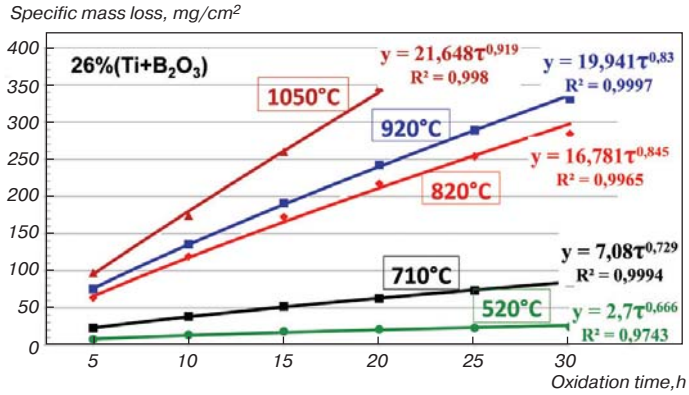

Fig. 13. Specific weight loss of composite electrode samples with initial charge composition {74C + 26(Ti + B_2O_3)} under isothermal conditions (520–1050 °C temperature range) in static air atmosphere

Table 3

Kinetic parameters found for the process of 74C + 26(Ti + B_2O_3) composite electrode samples oxidation

Oxid. temp., °C	K_T	a	R^2	$n = 1/a$	Limiting mode of oxidation
520	2.7	0.666	0.974	1.50	*D-K*
710	7.08	0.729	0.999	1.37	*D-K*
820	16.781	0.845	0.997	1.18	*D-K*
920	19.941	0.83	0.999	1.21	*D-K*
1050	21.648	0.919	0.998	1.09	K

Note: *K* – kinetic mode of oxidation reaction; *D-K* – mixed diffusional-kinetic mode of oxidation.

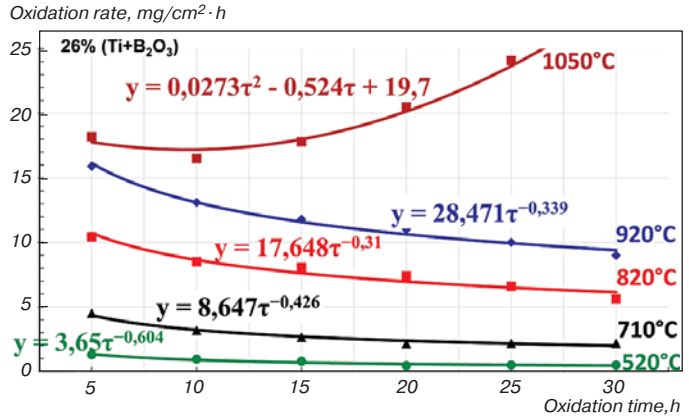

Fig. 14. Oxidation rate of composite electrode samples with {74C + 26(Ti + + B_2O_3)} initial charge composition under isothermal conditions (520–1050 °C) in static air atmosphere

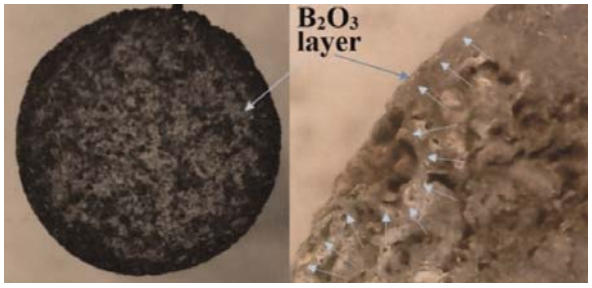

Fig. 15. Glassy B_2O_3 layer at the composite sample surface after its oxidation at 710 °C

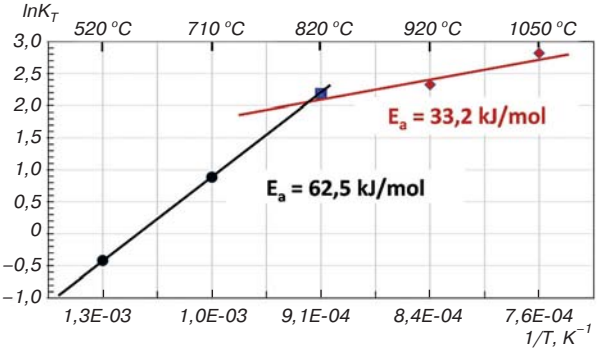

Fig. 16. Dependency $lnKp = f(1/T)$ for oxidation reaction of the composite synthesized from {74C + 26(Ti + B_2O_3)} initial charge

interval 520–1050 °C. These parameters depend upon oxidation temperature and prehistory of the studied composite C – TiC/TiB_2 synthesis (i.e., its initial charge), as namely TiC/TiB_2 fraction is a source of TiO_2 and B_2O_3 protective layers generation. A relatively high resistance to oxidation for various composites is generally due to the presence of simple and complicated amorphous and partially crystallized phases of Ti – C – B – O composition at the surface and between carbon grains in the volume. The oxidative resistance level for a definite composite mainly depends upon the quality of B_2O_3 surface layer formation and its rate of evaporation from the surface in cause of oxidation test. A relatively dense layer of glassy B_2O_3 at the surface does exist up to ~820 °C and this is the reason for a mixed oxidation mode including both oxygen diffusion and oxidation kinetics as constituents in the overall composite oxidation process with an effective E_a value ~62.5 kJ/mol. At a higher temperature — in the interval 820–1050 °C — the rate of B_2O_3 evaporation is increasing and the overall mode of oxidation process is changed to another one with an effective E_a = ~33.2 kJ/mol. Under these conditions the quantity of glassy B_2O_3 is supposed to be not enough to form a continuous layer at the composite surface which becomes to be covered with a non-uniform layer of titanium oxide (see **Fig. 17** and **Table 4**).

Temperature of running an oxidation test is reflected in the surface appearance of the corresponding composite samples **(Fig. 18)**.

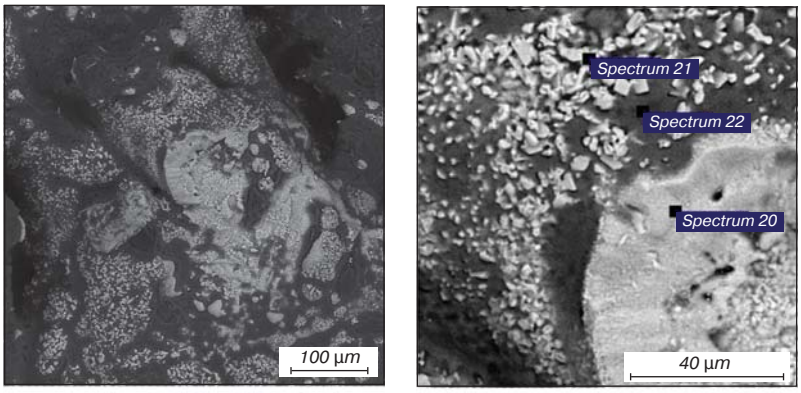

Fig. 17. SEM-EDX analysis results: the surface of {74C + 26(Ti + + B_2O_3)} composite after its oxidation in isothermal conditions at 920 °C for 30 h in static air atmosphere

Table 4

EDX local analysis results of {74C + 26(Ti + B_2O_3)} composite surface after oxidation test run at 920

No. of a local spectrum	Local composition for elements, atomic %				Possible phases
	Ti	C	B	O	
20	62.02	8.10	–	29.87	Ti – C – B – O
21	44.53	5.69	–	49.78	
22	1.98	–	29.61	68.41	

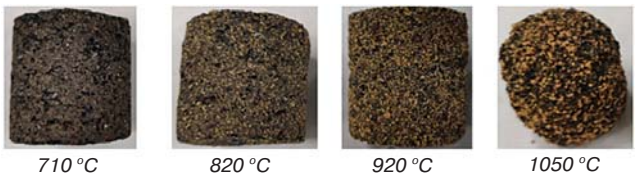

Fig. 18. Surface appearance of the composite samples of {74C + 26(Ti + + B_2O_3)} initial composition after oxidation runs for 30 h at various temperatures

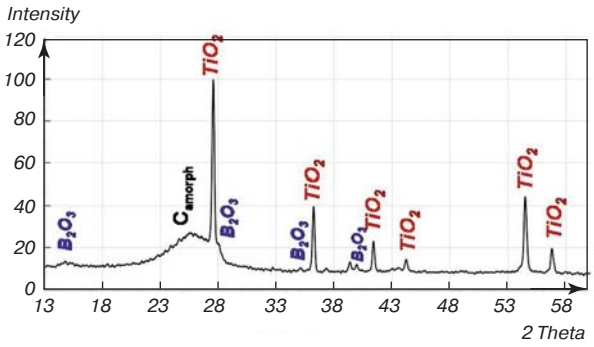

Fig. 19. XRD analysis results of {74C + 26(Ti + B_2O_3)} composite sample after a prolonged oxidation at 1050 °C for 30 hours

Surface color is transformed from almost black to orange-yellow with various combinations. The form and volume of composite samples remain almost unchanged at testing temperatures 710, 820 and 920 °C, whereas testing at 1050 °C is accompanied with shedding of carbon base and oxide layer in cause of the oxidation experiment. The powder fraction consists of the carbon base, titanium oxide and traces of boron oxide **(Fig. 19)**.

Conclusions

1. A novel technological scheme of composite electrode materials production is presented. The scheme is based upon a standard industrial procedure of graphite materials calcination.

2. Various composite electrode samples C – TiC/TiB_2 synthesized at 1050 °C in lab-scale conditions were proved to be highly stable in oxidizing media that are typical for working zones of arc steel-smelting and ore-thermal furnaces, magnesium cells and other metallurgical equipment.

3. A relatively high level of the composite resistance to oxidation is provided with the formation of simple and complicated amorphous phases of Ti – C – B – O system at the surface and in the inter-crystallite space between carbon grains. The level of a composite oxidation resistance can be controlled with glassy boron oxide layer generation and its further evaporation from the composite surface that is additionally protected with TiO – TiO_2 oxide phases.

4. An overall mechanism of C – MeC/MeB_2 composite oxidation is established and kinetic parameters of the corresponding oxidation reaction are found including effective activation energy and rate constant values for various experimental conditions.

5. The presented technology of composite electrodes production may be applied for synthesis of a wide range of C – MeC/MeB_2 composites for various applications including electrodes for aluminium cells.

References

1. Rudko V. A., Gabdulkhakov R. R., Pyagai I. N. Scientific and Technical Substantiation of the Possibility for the Organization of Needle Coke Production in Russia. *Journal of Mining Institute*. 2023. Vol. 263. pp. 795–809.

2. Nasifullina A. I., Starkov M. K., Gabdulkhakov R. R., Rudko V. A. Petroleum Coking Additive – Raw Material Component for Metallurgical Coke Production. Part 2. Experimental Studies of Obtaining a Petroleum Coking Additive. *CIS Iron Steel Review*. 2022. Vol. 24. pp. 9–16.

3. Sharikov F. Yu. Taking Into Account Convective Heat and Mass Exchange in Autoclave Reactors When Scaling Hydrothermal and Hydrometallurgical Processes. *Tsvetnye Metally*. 2022. No. 4. pp. 77–86.

4. Zubkova O. S., Alexeev A. I., Sizyakov V. M., Polyanskiy A. S. Research of Sulfuric Acid Salts Influence on Sedimentation Process of a Clay Suspension. *ChemChemTech*. 2022. Vol. 65, Iss.1. pp. 44–49.

5. Chukaeva M. A., Matveeva V. A., Sverchkov I. P. Complex Processing of High-Carbon Ash and Slag Waste. *Journal of Mining Institute*. 2022. Vol. 253. pp. 97–104.

6. Litvinenko V., Bowbrick I., Naumov I., Zaitseva Z. Global Guidelines and Requirements for Professional Competencies of Natural Resource Extraction Engineers: Implications for ESG Principles And Sustainable Development Goals. *Journal of Cleaner Production*. 2022. Vol. 338. 130530.

7. Bolobov V. I., Popov G. G. Methodology for Testing Pipeline Steels for Resistance to Grooving Corrosion. *Journal of Mining Institute*. 2021. Vol. 252. pp. 854–860.

8. Lebedev A. B., Utkov V. A., Khalifa A. A. Sintered Sorbent Utilization for H2S Removal from Industrial Flue Gas in the Process of Smelter Slag Granulation. *Journal of Mining Institute*. 2019. Vol. 237. pp. 292–297.

9. Vagapova E. A., Ivanov S. L., Ivanova P. V., Khudyakova I. N. Hydraulic Miner with Dewatering of Peat in Travelling Magnetic Field. *MIAB*. 2023. No. 7. pp. 21–36.

10. Zubkova O., Pyagay I., Pankratieva K., Toropchina M. Development of Composition and Study of Sorbent Properties Based on Saponite. *Journal of Mining Institute*. 2023. Vol. 259. pp. 21–29.

11. Nemchinova N. V., Konovalov N. P., Konovalov P. N., Doshlov I. O. Reducing the Environmental Impact of Aluminum Production Through the Use of Petroleum Pitch. *iPolytech Journal*. 2023. Vol. 27, Iss. 4. pp. 800–808.

12. Astapov A. N., Terentieva V. S. Review of Home-Grown Technologies in the Field of Protection of Carbon-bearing Materials from Gaseous Corrosion and Erosion in Plasma's High-Speed Flow. *Izvestiya Vuzov. Poroshkovaya Metallurgiya i Funktsional'nye Pokrytiya*. 2014. Iss. 4. pp. 50–70.

13. Dyskina B. Sh., Kabanova T. V. The Use of Man-Made Waste from the Ural Region to Protect Graphite Electrodes. *Advances in Chemistry and Chemical Technology*. 2014. Vol. 28, Iss. 10. pp. 39–41.

14. Lebedev V. A., Sedykh V. I. Metallurgy of Magnesium. Yekaterinburg: UGTU-UPI, 2010. 174 p.

15. Ren Y., Qian Y., Xu J., Jiang Y., Zuo J., Li M. Oxidation and Cracking/Spallation Resistance of ZrB_2–SiC–$TaSi_2$–Si Coating on Siliconized Graphite at 1500 °C in Air. *Ceramics International*. 2019. Vol. 46, Iss. 5. pp. 6254–6261.

16. Pat. RU No. 2522011 C1. Int. C25B 11/14. Method of Producing Graphitised Articles and Apparatus for Realising Said Method. Naumov N. A., Rybjanets I. V., Naprasnik M. M., Bogatyrev S. S. Appl. 09.01.2013, Publ. 10.07.2014, Bull. No. 19.

17. Schnittker A., Nawrocki H. Performance of Graphitized Carbon Cathode Blocks. *Light Metals*. 2003. pp. 641–645.

18. Pat. RU No. 2245396 C2. Int. C. 25 C3/08. Impregnated Graphite Cathode for Aluminum Electrolysis. Polyus R., Dreyfus J.-M. Appl. 01.02.2000, Publ. 27.01.2005, Bull. No. 3.

19. Feshchenko R. Yu., Eremin R. N., Erokhina O. O., Povarov V. G. Improvement of Oxidation Resistance of Graphite Blocks for the Electrolytic Production of Magnesium by Impregnation with Phosphate Solutions. Part 2. *Tsvetnye Metally*. 2022. No. 1. pp. 24–29.

20. Fekri M., Jafarzadeh K., Khalife Soltani S. A., Valefi Z., Mazhari Abbasi H. Improvement of Oxidation Resistance of Graphite by Aluminosilicate Coating with Aluminum Metaphosphate Interlayer. *Carbon Letters*. 2023. Vol. 33. pp. 2095–2108.

21. Eremin R. N. Increasing the Resistance of Graphitized Anodes of Magnesium Electrolyzers to High-Temperature Oxidation. Abstract of Diss. ... Candidate of Technical Sciences. St. Petersburg, 2021. 22 p.

22. Merkov S. M., Alekseev A. V., Kinshpont E. R., Milinchuk V. K., Lainer Yu. A., Samoilov E. N. Investigation Into the Impregnation of Roasted Anodes of Aluminum Electrolyzers. *Izvestiya Vuzov. Tsvetnaya Metallurgiya*. 2015. Iss. 3. pp. 16–21.

23. Arai Y., Inoue R., Goto K., Kogo Y. Carbon Fiber Reinforced Ultra–High Temperature Ceramic Matrix Composites: a Review. *Ceramics International*. 2019. Vol. 45, Iss. 12. pp. 14481–14489.

24. Nikolaev A. N. Synthesis and Study of Glass-Ceramic Compositions Modified with Oxides and Carbon-Containing Materials. Abstract of Diss. ... Candidate of Technical Sciences. St.Petersburg, 2023. 20 p.

25. Dyskina B. Sh., Lesyuk V. S., Kabanova T. V. Optimization of the Composition of the Protective Coating Against High-Temperature Oxidation of Graphite Electrodes. *Chemistry and Chemical Technology*. 2015. Vol. 58, Iss. 7. pp. 53–55.

26. Pat. CN No. 107043276. Graphite Electrode Protection Method. Huang Jiaxu, Cheng Xiaozhe, Wang Tanglin. Publ. 15.08.2017.

27. Pat. RU No. 2788294 C1. In t. C25B 11/04; H05B 7/085 Method of Protection of Graphite Electrodes from High-Temperature Oxidation. Erokhina O. O., Feshchenko R. Yu., Pirogova N. A., Eremin R. N. Appl. 28.06.2022, Publ. 17.01.2023, Bull. No. 2.

28. Yang H., Zhao H.-S., Li Z.-Q., Liu X.-X., Zhang K.-H., Wang T.-W., Liu B. Review of Oxidant Resistant Coating on Graphite Substrate of HTR Fuel Element. *Journal of Central South University*. 2019. Vol. 26, Iss. 11. pp. 2915–2929.

29. Pat. CN No. 110002839.. Oxidation Resisting Coating Material for Graphite Electrode in Electric Furnace Smelting. Chao Shangkui, Li Lixiang, Xiao Xiaoshuai. Publ. 12.07.2019.

30. Askerbekov S. K., Chikhray E. V., Ponkratov Yu. V., Nikitenkov N. N. Research on High-Temperature Corrosion of SiC-coating on Graphite. *Bulletin of Tomsk Polytechnic University. Geo Assets Engineering*. 2019. Vol. 330, Iss. 6. pp. 98–108.

31. Pat. RU 2613397 C1. Int. C04B 35/58. Method of Protective Coating Manufacturing. Bankovskaya I. B., Kolovertnov D.V., Sazonova M. V. Appl. 03.12.2015, Publ. 16.03.2017, Bull. No. 8.

32. Wang P., Li H., Ren X., Yuan R., Hou X., Zhang Yu. HfB2 – SiC – MoSi2 Oxidation Resistance Coating Fabricated Through in-Situ Synthesis for SiC Coated C/C Composites. *Journal of Alloys and Compounds*. 2017. Vol. 722. pp. 69–76.

33. Pat. US S6632762 B1. Int. Cl. C04B 35/565. Oxidation Resistant Coating for Carbon. Zaykoski J. A., Talmy I. G., Ashkenazi K. J. Appl. 15.11.2001, Publ. 14.10.2003.

34. Li T., Johansen S. T., Solheim A. Uneven Cathode Wear in Aluminium Reduction Cells. *Light Metals*. 2016. pp. 927–932.

35. Novak B., Ratvik A. P., Wang Zh., Grande T. Formation of Aluminium Carbide in Hall-Héroult Electrolysis Cell Environments. *Light Metals*. 2018. pp. 1215–1222.

36. Landry J.-R., Fini M. F., Soucy G., Désilets M., Pelletier P., Rivoaland L., Lombard D. Laboratory Study of the Impact of the Cathode Grade on the Formation of Deposits on the Cathode Surface in Hall-Héroult Cells. *Light Metals*. 2018. pp. 1229–1233.

37. Kofstad P. Deviation from Stoichiometry, Diffusion and Electrical Conductivity in Simple Metal Oxides. Moscow: Mir, 1975. 396 p.

38. Pat. RU 2814568 C1. Int. C04B 35/532, C04B 35/56, C04B 35/58. A Method for Producing Carbon-based Composite Materials. Gorlanov E. S., Mushikhin E. A. Appl. 15.05.2023, Publ. 01.03.2024, Bull. No. 7.

NFM